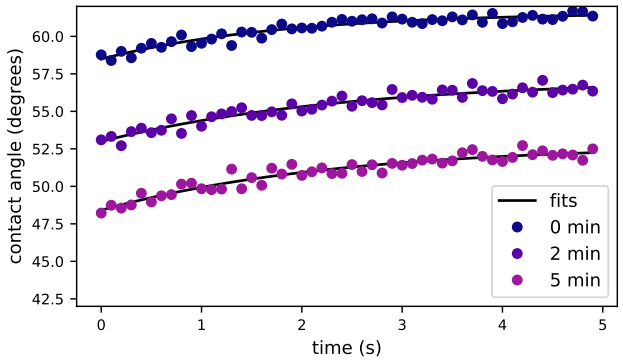

FIG. 13. Contact angle versus time for the same experiments shown in Fig. 4a, limited to the constant-volume relaxation region of the experiment. Fits shown are for exponential decay.

SUPPLEMENTAL INFORMATION

Relaxation experiments

The contact angle in the relaxation experiments of Fig. 4a decay exponentially in time as seen in Fig. 13. Exponential relaxation can be derived from overdamped dynamics near a stable equilibrium point. When $q = 0$, Eq. 3 simplifies to

$$\dot{w} = -\frac{w}{3h}\frac{\partial h}{\partial \theta}\dot{\theta} = -\alpha\dot{\theta}. \tag{8}$$

When the changes in θ and w are small, the prefactor, $\alpha \equiv (w/3h)\partial h/\partial\theta$, is approximately constant over the course of the relaxation. We also expand $\cos(\theta) - \cos(\theta_{eq}) \approx \sin(\theta_{eq})(\theta_{eq} - \theta)$. Applying the overdamped assumption of Eq. 4, $F = \beta\dot{w}/2$, we find

$$\dot{\theta} = -\frac{2\gamma\sin(\theta_{eq})}{\alpha\beta}(\theta_{eq} - \theta). \tag{9}$$

We can solve directly for $\theta(t)$:

$$\theta(t) \approx \theta_{eq} - (\theta_{eq} - \theta_0)\exp(-\frac{2\gamma\sin(\theta_{eq})}{\beta\alpha}t), \tag{10}$$

where θ_0 is the contact angle at time $t = 0$. Thus, by fitting $q = 0$ relaxation with an exponential, one can find β and θ_{eq} directly.

Figure 7 shows β versus flow rate, q, for the experiments shown in Fig. 4b.

Additional data

Figure 14 shows the same data sets shown in Fig. 2 of the main text as a function of time. Time has been roughly offset to align the early stages of different experiments. These plots show an initial pinned (constant width) configuration where the contact angle decreases quickly, followed by a decreasing width and hence slower contact angle decrease.

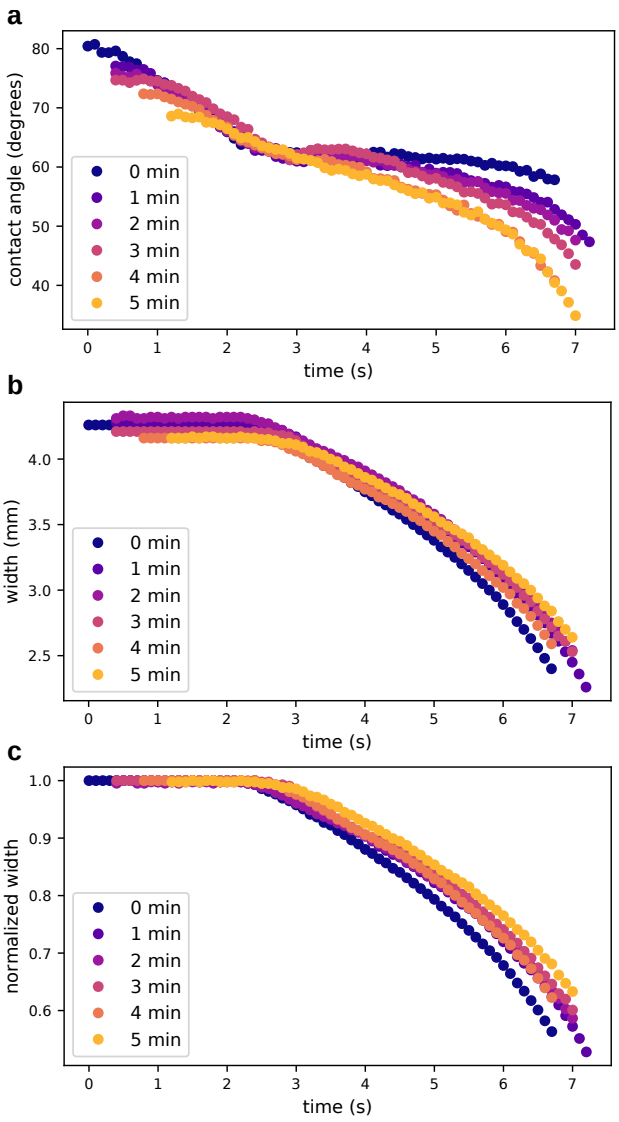

FIG. 14. (a) Contact angle as a function of time for the same experiments shown in Fig. 2. (b) Drop width as a function of time for the same set of experiments. Small variations in the initial width make it difficult to compare experiments. (c) As in (b), but with the widths for each experiment normalized by the initial pinned width for that experiment. In all panels, experiments have been shifted left-right to roughly align the initial (pinned) contact angle measurements.

Figure 15 shows all three sets of wait-time experiments, all three sets of $\tau \approx 0$ flow-rate experiments, and all three sets of $\tau = 3$ minutes flow-rate experiments for water on silanized glass with best-fit model curves overlaid. Each row shows data taken on a different days under the same conditions. These figures show that although there is considerable day-to-day variation of the equilibrium contact angles and damping coefficients, the trends as to how

they vary with wait time, τ, and flow rate, q, as reported in the text are consistent for all cases.

Figure 16 shows all experiments as above for water on gold. Fig. 17 shows all experiments for toluene on silanized glass.

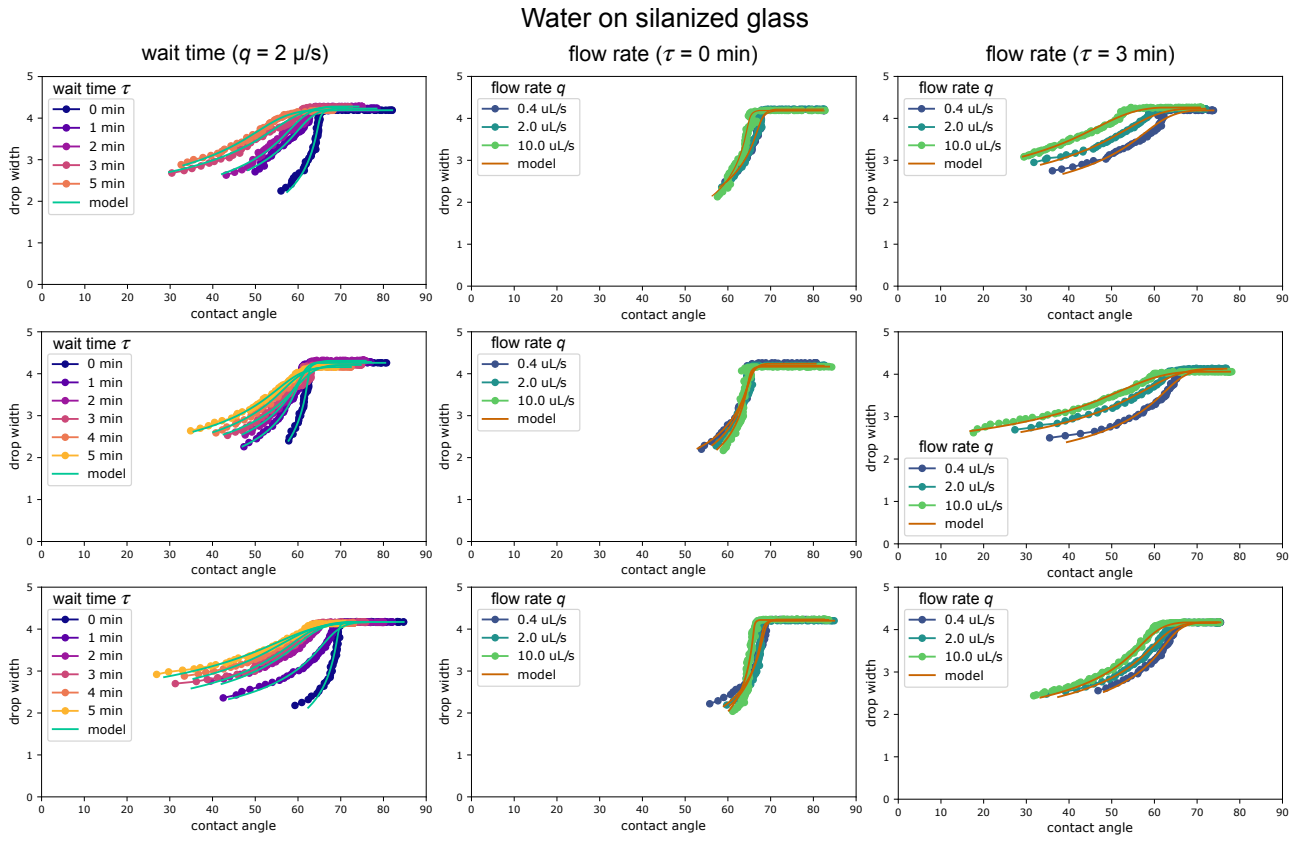

FIG. 15. Drop width, w versus contact angle, θ for water on silanized glass. The best-fit model curves are overlaid. Left column shows data at the wait times, τ, in the legend with $q = 2$ μL/s. The middle and right columns show data at the flow rates, q, given in the legend. Middle column shows data for $\tau \approx 0$ minutes, and right column shows data for $\tau = 3$ minutes. Experiments on different rows were done on different days under the same conditions. Although there is considerable day-to-day variation of the equilibrium contact angles and damping coefficients, the trends as reported in the main text are consistent for all cases.

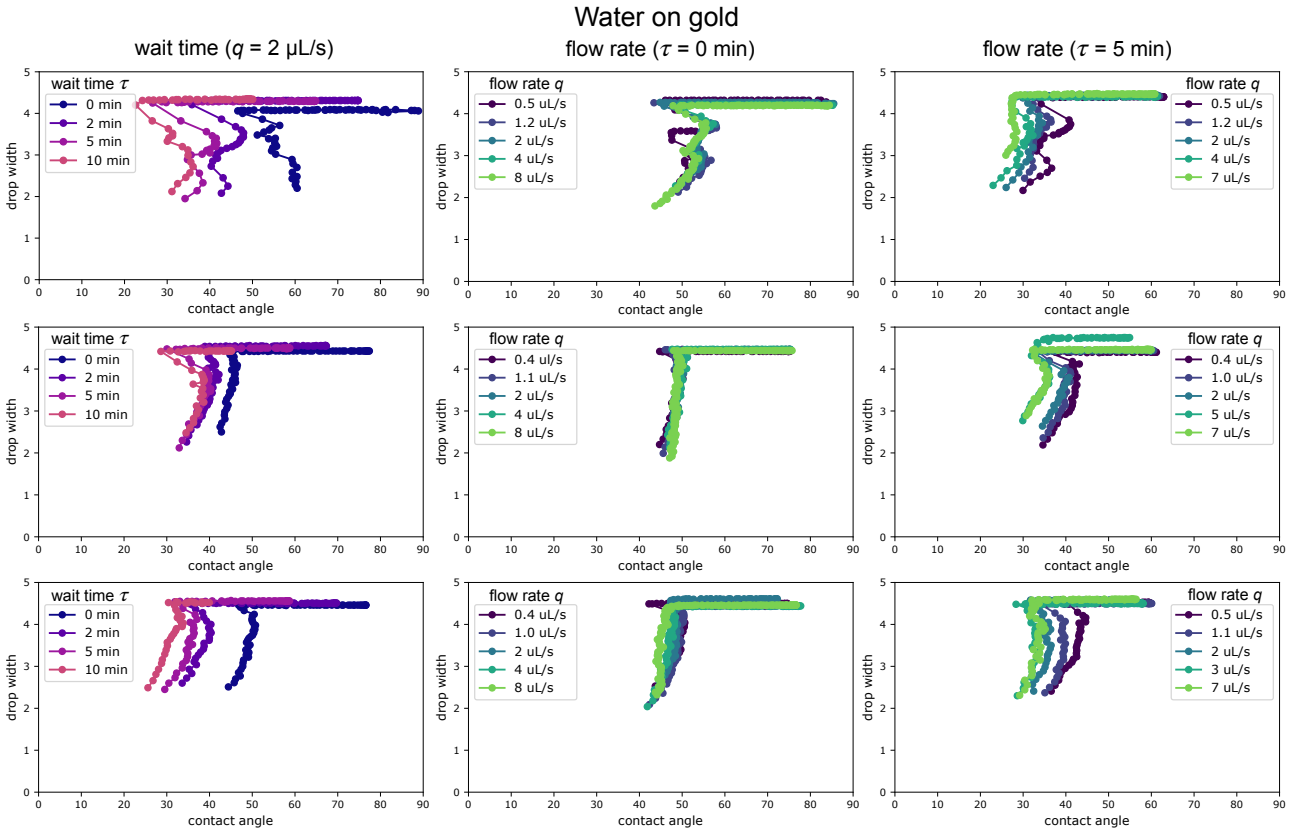

FIG. 16. Drop width, w versus contact angle, θ for water on gold. Left column shows data at the wait times, τ, in the legend with $q = 2$ μL/s. The middle and right columns show data at the flow rates, q, given in the legend. Middle column shows data for $\tau \approx 0$ minutes, and right column shows data for $\tau = 5$ minutes. Experiments on different rows were done on different days under the same conditions.

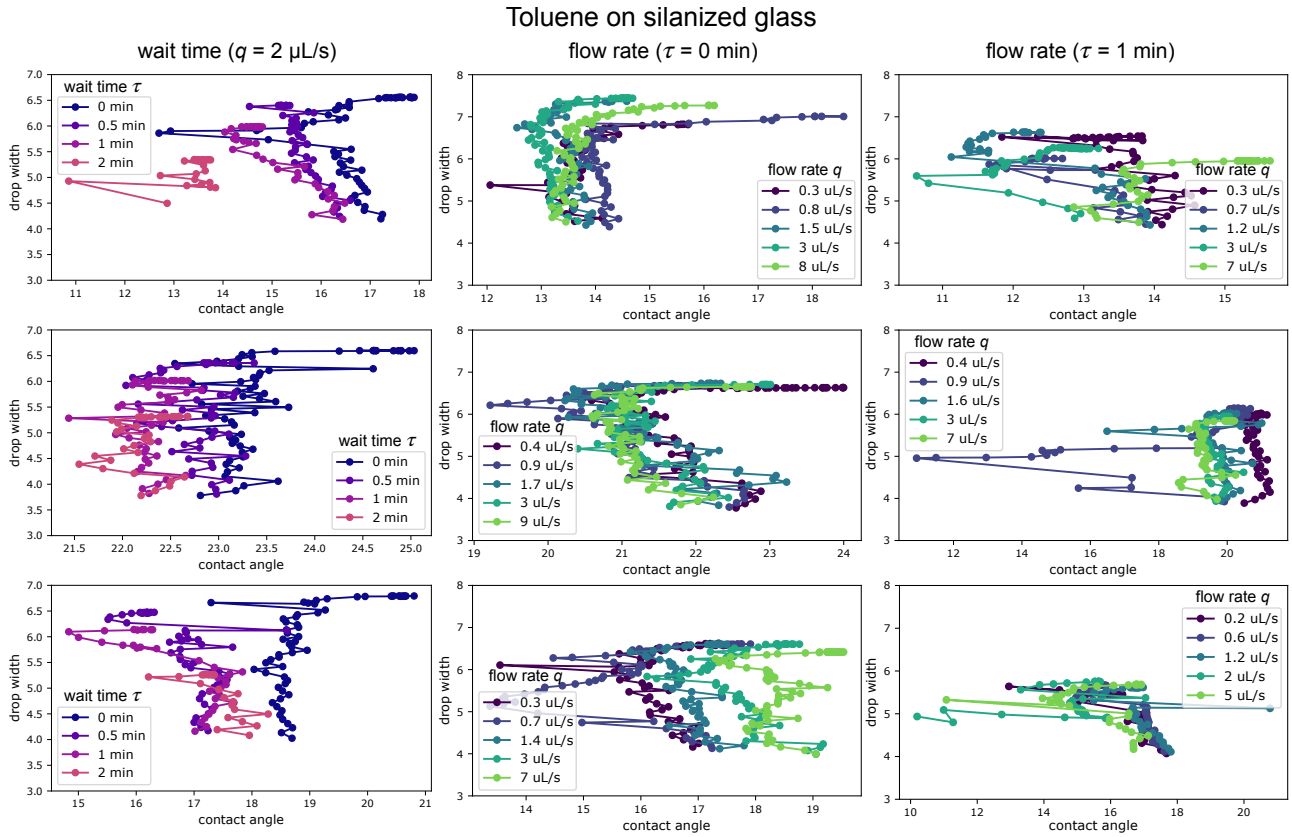

FIG. 17. Drop width, w versus contact angle, θ for toluene on silanized glass. Left column shows data at the wait times, τ, in the legend with $q = 2$ μL/s. The middle and right columns show data at the flow rates, q, given in the legend. Middle column shows data for $\tau \approx 0$ minutes, and right column shows data for $\tau = 5$ minutes. Experiments on different rows were done on different days under the same conditions.